Ultrasensitive and Selective Electrochemical Diagnosis of Breast Cancer Based on a Hydrazine-Au Nanoparticle-Aptamer Bioconjugate

ARTICLE *in* ANALYTICAL CHEMISTRY · DECEMBER 2012

Impact Factor: 5.64 · DOI: 10.1021/ac302923k · Source: PubMed

3 AUTHORS, INCLUDING:

Ye Zhu
Shandong University
10 PUBLICATIONS **172** CITATIONS
SEE PROFILE

Dr. Pranjal Chandra
Indian Institute of Technology Guwahati
33 PUBLICATIONS **327** CITATIONS
SEE PROFILE

analytical chemistry

Article

pubs.acs.org/ac

Ultrasensitive and Selective Electrochemical Diagnosis of Breast Cancer Based on a Hydrazine–Au Nanoparticle–Aptamer Bioconjugate

Ye Zhu,[†] Pranjal Chandra, and Yoon-Bo Shim*

Department of Chemistry and Institute of Bio-Physico Sensor Technology, Pusan National University, Busan 609-735, South Korea

Supporting Information

ABSTRACT: Human epidermal growth factor receptor 2 (HER2) and HER2-overexpressing breast cancer cells were detected using an electrochemical immunosensor combined with hydrazine and aptamer-conjugated gold nanoparticles (AuNPs). The sensor probe was fabricated by covalently immobilizing anti-HER2 onto a nanocomposite layer that was composed of self-assembled 2,5-bis(2-thienyl)-1*H*-pyrrole-1-(*p*-benzoic acid) (DPB) on AuNPs. The hydrazine–AuNP–aptamer bioconjugate, where the hydrazine reductant was directly attached onto AuNPs to avoid the nonspecific deposition of silver on the sensor surface, was designed and used to reduce silver ion for signal amplification selectively. The silver-stained target cells were visualized easily by the bare eye and an optical microscope, and the cells were quantitatively analyzed using stripping voltammetry. The parameters affecting the analytical response were optimized. The proposed sensor was capable of differentiating between HER2-positive breast cancer cells and HER2-negative cells. This method exhibited an excellent diagnosis method for the ultrasensitive detection of SK-BR-3 breast cancer cells in human serum samples with a detection limit of 26 cells/mL.

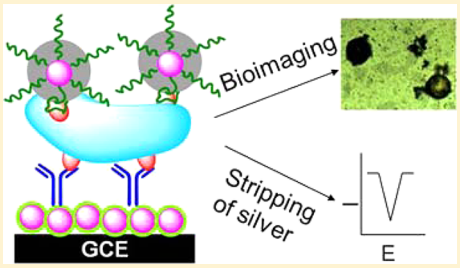

Human epidermal growth factor receptor 2 (HER2), which is overexpressed in 10–25% of breast cancers,[1] is a key prognostic marker and an effective therapeutic treatment target for breast cancer.[2] The overwhelming evidence from numerous studies indicates that patients with HER2-positive breast cancer have a worse prognosis than patients with HER2-negative breast cancer, and it requires a special therapy.[3,4] Therefore, identifying the overexpression of HER2 for breast cancer diagnosis and therapy is critical. Recently, several methods for detecting HER2-positive cancer cells have been developed, which include colorimetry,[5] fluorescence,[6] scattering assays,[7] and cell imaging.[8] Most of these techniques are limited to cell detection and are not available for measuring the concentration of serum HER2, which offers a far less invasive method of determining the HER2 status than a biopsy. Large clinical trials have clearly shown that the best predictive HER2 testing strategy is associated with practical and economic issues.[9] Thus, the development of a convenient, cost-effective method for the detection of both the HER2 protein and HER2-overexpressing cells is desirable. To date, electrochemical sensors have been widely used in point-of-care devices due to the advantages of being portable, simple, easy to use, cost-effective, and disposable;[10] however, electrochemical sensors for the detection of HER2-overexpressing cancer cells[11] have not been reported. This study aims to develop electrochemical and microscopic methods combined with a gold nanoparticle (AuNP)-based bioconjugate for the simple and reliable detection of both HER2 protein and HER2-overexpressing SK-BR-3breast cancer cells

In the past decade, the silver deposition method on nanomaterials (AuNPs or graphene) has been used for the detection of DNA and proteins.[12−14] In these assays, silver ions are chemically reduced onto the sensor surface using a reductant (e.g., hydroquinone) without discrimination between the target molecules (or bioconjugates) and the sensor surfaces, where the nonspecific deposition of silver on the whole sensor surface might result in irreproducibility. Thus, to overcome nonspecific deposition of silver on the target molecules, we proposed a new method for silver reduction without using an external reductant. For this purpose, we tried to use the reductant-attached bioconjugate for the exclusive deposition of silver on the target molecules and also to use the conjugate to achieve accurate detection of breast cancer cells and a protein biomarker as a model case. In this strategy, since the reductant is directly bonded onto the electrode surface through the bioconjugate immunocomplex, controlled and selective silver reduction and deposition is possible. Silver enhancement through hydroquinone has been used previously to detect protein, antibody, and DNA-conjugated gold nanoparticles in histochemical electron microscopy studies[15,16] and DNA hybridization assays,[12] but the hydrazine-attached bioconjugate method for the direct detection of cancer cells and proteins has not been reported.

Herein, hydrazine acts as a reductant which has the capability of reducing silver ion to silver metal,[17] and it is attached to

Received: October 9, 2012
Accepted: December 5, 2012
Published: December 5, 2012

AuNPs to make a bioconjugate of hydrazine−AuNP−aptamer (Hyd−AuNP−Apt), where the aptamer is specific toward HER2. The sensor probe is fabricated by covalently immobilizing the monoclonal anti-HER2 onto the nanocomposite, which comprises self-assembled 2,5-bis(2-thienyl)-1*H*-pyrrole-1-(*p*-benzoic acid) (DPB) and AuNPs. During the detection process, the anti-HER2-immobilized probe, HER2 or HER2-overexpressing SK-BR-3 breast cancer cells, and Hyd−AuNP−Apt bioconjugate make a sandwich-type structure. The silver ion is selectively reduced by hydrazine and specifically deposits onto the Hyd−AuNP−Apt bioconjugate, which is reacted with the HER2 or HER2-overexpressing SK-BR-3 breast cancer cells. The deposited silver is observed using a microscope and is analyzed using square wave stripping voltammetry (SWSV) to determine the amount of HER2 or HER2-overexpressing cells. This is the first report in which breast cancer cells have been silver stained selectively through interaction with the Hyd−AuNP−Apt bioconjugate and observed directly with the bare eye and under a microscope.

EXPERIMENTAL SECTION

Materials. A monomer bearing a benzoic acid group, DPB, was synthesized using a previously reported method.[18] Monoclonal anti-HER2 from mouse and HER2 protein were purchased from Abcam (Cambridge, MA). A 3′-thiolated RNA aptamer (SE15-8, 3′-AAAAGTTGTGAGGGGAGGGA-TAGGGTAGGGCACGACTAGTCAAGAAAATG-5′) that is specific to HER2[19] was obtained from the Bioneer Corp. (South Korea). SK-BR-3, MCF10, MCF7, and Hela cell samples were obtained from the Korean Cell Line Bank (South Korea). Bovine serum albumin (BSA), hydrazine sulfate, silver nitrate, 1-ethyl-3-[3-(dimethylamino)propyl]-carbodiimide (EDC), *N*-hydroxysuccinimide ester (NHS), gold(III) chloride trihydrate, sodium citrate, and sodium borohydride ($NaBH_4$) were obtained from Sigma-Aldrich (St. Louis, MO). Tetrabutylammonium perchlorate (TBAP; electrochemical grade) was obtained from Fluka and purified using the conventional method, followed by drying under vacuum at 10^{-5} Torr. Phosphate-buffered saline (PBS) solutions were prepared with 0.01 M disodium hydrogen phosphate (Aldrich), 0.01 M sodium dihydrogen phosphate (Aldrich), and 0.9% sodium chloride (Sigma). TE buffer, which was prepared with 10 mM tris(hydroxymethyl)aminomethane and 1 mM ethylenediaminetetraacetic acid and adjusted to a pH of 8.0 with HCl, was used to dilute the aptamer. RPMI 1640 medium, fetal bovine serum (FBS), trypsin−EDTA, penicillin/streptomycin, and Hank's balance salt (HBS) solution were purchased from Sigma-Aldrich. All other chemicals were of extrapure analytical grade and used without further purification. Deionized water (18 MΩ cm) from a Direct-Q system (Millipore, Billerica, MA) was used to prepare all aqueous solutions.

Apparatus. The modified glassy carbon electrode (GCE) (area 0.07 cm^2), Ag/AgCl (in saturated KCl), and a platinum (Pt) wire were used as the working, reference, and counter electrodes, respectively. The indium tin oxide-coated glass (ITO glass) was purchased from Sigma-Aldrich. Cyclic voltammetry (CV) and SWSV were performed using a KST-P1 potentiostat/galvanostat, Kosentech (South Korea), and an EG&G PAR model 273A. Microscopic images were obtained using an Optika microscope, M-068. Scanning electron microscopy (SEM) images were obtained using a Cambridge Stereoscan 240. X-ray photoelectron spectroscopy (XPS) experiments were performed using a VG Scientific ESCA Lab 250 XPS spectrometer coupled with a monochromatic Al Kα source with charge compensation at the Korea Basic Science Institute (Busan, South Korea).

Preparation of the Self-Assembled DPB(AuNP). Self-assembled DPB(AuNP) was prepared according to the previously reported method.[20] At first 50 mL of 0.01 wt % $HAuCl_4$ in H_2O was mixed with 1 mL of 38.8 mM trisodium citrate. After 1 min, 0.5 mL of a freshly prepared $NaBH_4$ solution was slowly added to the mixture. During the addition of $NaBH_4$, the color of the resulting solution turned from yellow to pink, indicating the formation of AuNPs.[21] In addition, a monomer solution was prepared by dissolving 1.0 mM DPB into a 0.1 M TBAP/acetonitrile solution, which exhibited a yellow color. Then the AuNP solution and the DPB monomer solution were mixed in a 1:1 ratio. The resulting solution turned blue, reflecting the self-assembly of the DPB monomer on the surface of AuNPs.

Preparation of the Hyd−AuNP−Apt Bioconjugate. The synthesized AuNPs were mixed with 2.23 nmol of the thiolated aptamer and incubated for 12 h at 4 °C to obtain aptamer-modified AuNPs through the formation of a Au−S bond. Then the unreacted thiolated aptamer was removed by centrifugation (13 000 rpm) for 15 min. The supernatant was removed, and the precipitate was washed three times with PBS. The washed precipitate was added to a 10 mM hydrazine sulfate solution and maintained at 4 °C for 12 h. As a result, hydrazine was attached to the surface of the AuNPs through electrostatic interactions. The mixture was centrifuged for 15 min to remove the excess hydrazine. The supernatant was removed, and the deposit was washed three times with PBS. The resulting Hyd−AuNP−Apt bioconjugate was dispersed in a 0.1 M PBS solution for further use.

Fabrication of the Probe. The fabrication of the probe is illustrated in Scheme 1. Before modification of the GCE, it was polished to a mirror finish with alumina slurry (0.3 and 0.05

Scheme 1. Schematic Representation of the Immunosensor for Detection of HER2 Protein and HER2-Overexpresing SK-BR-3 Breast Cancer Cells[a]

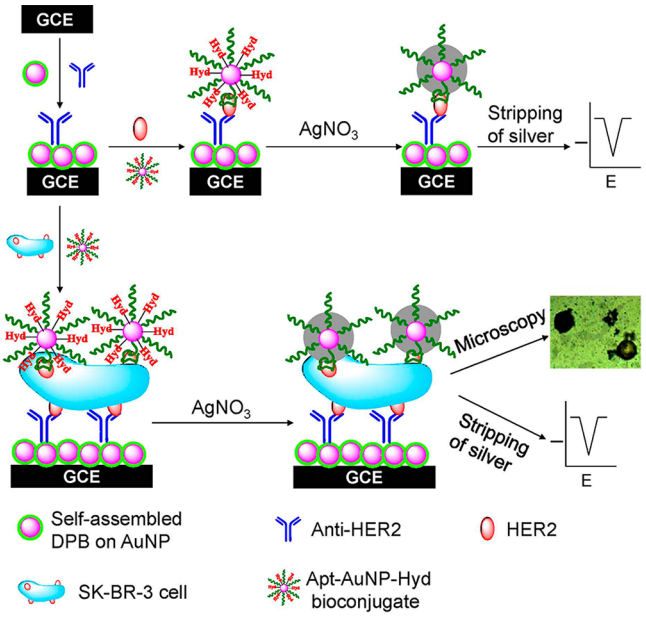

[a]Microscopic images were observed on ITO glass instead of the GCE.

dx.doi.org/10.1021/ac302923k | *Anal. Chem.* 2013, 85, 1058−1064

μm, respectively), followed by ultrasonication for 15 s to remove the alumina particles, and then rinsed with double-distilled water and ethanol, respectively. The electropolymerization was then performed in the self-assembled DPB(AuNP) solution by potential cycling two times between 0.0 and +1.0 V (vs Ag/AgCl) at 100 mV/s to form a poly-DPB(AuNP) nanocomposite film on the electrode surface, followed by rinsing with acetonitrile to remove the excess chemicals from the electrode surface. Thereafter, the poly-DPB(AuNP) nanocomposite-covered electrode was activated using an EDC/NHS solution for 4 h at room temperature, followed by washing with PBS. Then the appropriate concentration of anti-HER2 solution (5 μL) was drop coated onto the activated electrode surface and incubated overnight at 4 °C. As a result, anti-HER2 was immobilized onto the poly-DPB(AuNP) nanocomposite through the formation of covalent bonds between the $-NH_2$ groups of anti-HER2 and the −COOH groups of the poly-DPB. After being washed with PBS, the anti-HER2-immobilized electrode was immersed into a 2% BSA solution for 30 min to block the unreacted sites. Finally, the anti-HER2/poly-DPB(AuNP)/GC probe was washed with PBS and used to detect HER2 and SK-BR-3 breast cancer cells.

Detection of HER2. To detect HER2, the anti-HER2-immobilized probe was immersed into 25-fold-diluted human serum containing HER2 for the appropriate time at 4 °C. HER2 in the solution was recognized and captured by the anti-HER2 immobilized on the electrode. Following the immunoreaction, the HER2-captured sensor was washed with 0.1 M PBS and then immersed into the PBS containing the Hyd−AuNP−Apt bioconjugate for 20 min at 35 °C. Through this step, the specific aptamer on the bioconjugate can recognize and bind with HER2. After being washed with PBS, the modified sensor was transferred into a 10 mM silver nitrate solution for 30 min. With AuNP acting as a catalyst, silver ion in the silver nitrate solution was reduced to silver metal by hydrazine on the Hyd−AuNP−Apt bioconjugate and subsequently deposited onto the bioconjugate. Then the final sensor was washed with distilled water and placed into an electrochemical cell that contained 0.1 M PBS (pH 7.0) as a measuring solution for the electrochemical tests. CV was recorded between 0 and 0.6 V at a scan rate of 50 mV/s, and SWSV was carried out from 0.0 to 0.6 V under the following conditions: step potential, 4 mV; amplitude, 25 mV; frequency, 15 Hz.

Culture and Detection of Cells. The breast cancer cell lines SK-BR-3 and MCF 7, normal breast cell line MCF 10A, and cancer cell line Hela were trypsinized, suspended in 20 mL of differentiation medium that contained 10% heat-inactivated fetal bovine serum, 100 units/mL penicillin, and 100 units/mL streptomycin, and cultured in 75 cm^2 tissue culture flasks at 37 °C under 5% CO_2/95% O_2 in a humidified incubator. The medium was replaced every two days. To detect the cells using the fabricated probe, the cells were resuspended in the human serum, which was diluted 25-fold with PBS. The detection of the breast cancer cells was first investigated using microscopy. Anti-HER2 was immobilized on the poly-DPB(AuNP)-coated ITO glass electrode and was used to detect the cells. After incubation with the cells, the resulting electrode was treated with the Hyd−AuNP−Apt bioconjugate and silver nitrate solution, respectively. After washing, the deposition of silver onto the captured cells was observed using microscopy. To quantitatively detect the cells, the anti-HER2/poly-DPB(AuNP)/GC probe was used to sequentially interact with the cell solution, the Hyd−AuNP−Apt bioconjugate, and the silver nitrate solution. Finally, the determination of the cells was performed by stripping the deposited silver from the modified electrode in PBS.

RESULTS AND DISCUSSION

Characterization of the Probe. The SEM images of poly-DPB/GC, poly-DPB(AuNP)/GC, anti-HER2/poly-DPB-(AuNP)/GC, and silver-deposited Hyd−AuNP−Apt/HER2/anti-HER2/poly-DPB(AuNP)/GC are displayed in the Supporting Information, Figure S1. A smooth film is observed for the poly-DPB/GC surface, which was prepared in a 0.05 M TBAP/acetonitrile solution containing 0.5 mM DPB monomer without AuNPs (image a), whereas particles are observed in the image of the poly-DPB(AuNP) nanocomposite, which was formed in a 0.05 M TBAP/acetonitrile solution containing 0.5 mM self-assembled DPB on AuNPs (image b). The diameter of these particles is approximately 10 nm, which is similar to that in a previous report.[15] The SEM image obtained for anti-HER2/poly-DPB(AuNP)/GC exhibits clusters of immobilized anti-HER2 on the surface of poly-DPB(AuNP)/GC (image c). For the final silver-deposited Hyd−AuNP−Apt/HER2/anti-HER2/poly-DPB(AuNP)/GC (image d), the surface appears rough because of the deposition of reduced silver onto the Hyd−AuNP−Apt bioconjugate.

To further confirm the modification of the electrode surface, XPS experiments were performed for poly-DPB(AuNP)/GC, anti-HER2/poly-DPB(AuNP)/GC, Hyd−AuNP−Apt/HER2/anti-HER2/poly-DPB(AuNP)/GC, and silver-deposited Hyd−AuNP−Apt/HER2/anti-HER2/poly-DPB(AuNP)/GC, as shown in Figure 1. All XPS spectra were referenced to the C

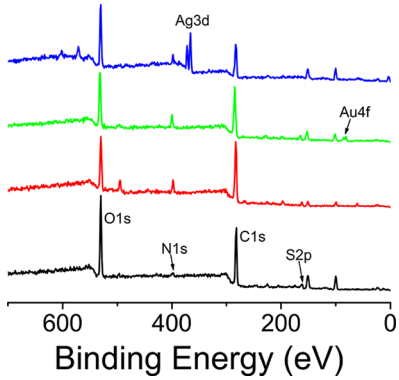

Figure 1. X-ray photoelectron spectra for (a, black) poly-DPB-(AuNP)/GC, (b, red) anti-HER2/poly-DPB(AuNP)/GC, (c, green) Hyd−AuNP−Apt/HER2/anti-HER2/poly-DPB(AuNP)/GC, and (d, blue) silver-deposited Hyd−AuNP−Apt/HER2/anti-HER2/poly-DPB(AuNP)/GC.

1s peak at 284.6 eV as an internal standard. The C peak and the O peak are observed for all surfaces. For the poly-DPB-(AuNP)/GC surface, a S 2p peak and a small N 1s peak, which are attributed to poly-DPB, are observed at 164.2 and 400.2 eV, respectively (spectrum a). Because the AuNPs are covered with the self-assembled poly-DPB, the Au peak does not appear in the XPS spectrum for poly-DPB(AuNP)/GC, as previously reported.[22] As observed in spectrum b, the intensity of the N 1s peak increases due to the amide bond formation between $-NH_2$ groups of anti-HER2 and −COOH groups of poly-DPB(AuNP)/GC, which indicates the successful immobilization of anti-HER2. In the Hyd−AuNP−Apt/HER2/anti-

dx.doi.org/10.1021/ac302923k | Anal. Chem. 2013, 85, 1058−1064

HER2/poly-DPB(AuNP)/GC spectra, small Au 4f peaks, which are related to the AuNP in the Hyd−AuNP−Apt bioconjugate, appear at 81.6 and 84.8 eV (spectrum c). After silver deposition, clearly distinguishable Ag 3d peaks appears at 367.7 and 373.7 eV, and the Au 4f peaks that were observed before silver deposition disappear (spectrum d), indicating that silver is successfully deposited onto the Hyd−AuNP−Apt bioconjugate.

Electrochemical Measurements. To confirm the modification of the sensor, cyclic voltammograms were recorded for each step in 0.1 M PBS, as shown in Figure 2. Because there

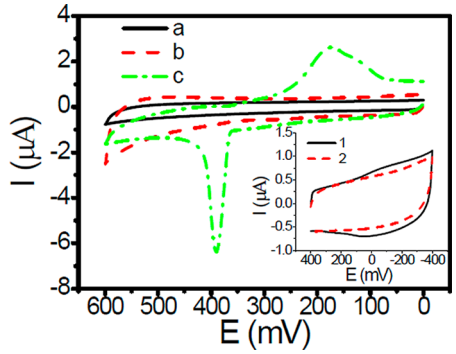

Figure 2. Cyclic voltammograms recorded for (a) the probe of anti-HER2/poly-DPB(AuNP)/GC, (b) silver nitrate-treated AuNP−Apt/HER2/anti-HER2/poly-DPB(AuNP)/GC, and (c) silver nitrate-treated Hyd−AuNP−Apt/HER2/anti-HER2/poly-DPB(AuNP)/GC in 0.1 M PBS (pH 7.0). Inset: cyclic voltammograms recorded for (1) Hyd−AuNP−Apt/HER2/anti-HER2/poly-DPB(AuNP)/GC and (2) AuNP−Apt/HER2/anti-HER2/poly-DPB(AuNP)/GC in 0.1 M PBS (pH 7.0).

were no electroactive species on the anti-HER2/poly-DPB-(AuNP)/GC probe, the recorded cyclic voltammogram does not exhibit any peaks in the potential range (Figure 2a). After the probe sequentially interacted with HER2 and the Hyd−AuNP−Apt bioconjugate, the attachment of hydrazine on the bioconjugate was confirmed and characterized by recording the cyclic voltammogram between +0.4 and −0.4 V in 0.1 M PBS. As expected, a pair of redox peaks of hydrazine are observed at 0.04/−0.08 V (curve 1 of the inset in Figure 2),[22,23] indicating that the sensor is capable of binding with HER2 and the Hyd−AuNP−Apt bioconjugate is successfully prepared. Then Hyd−AuNP−Apt/HER2/anti-HER2/poly-DPB(AuNP)/GC was immersed into a silver nitrate solution for 30 min, followed by washing with distilled water; a cyclic voltammogram was then recorded in 0.1 M PBS (Figure 2c). A pair of redox peaks related to Ag/Ag^{I} are clearly observed at +0.39/+0.17 V,[24] which indicates that the silver ion in the solution was successfully reduced to silver metal and deposited onto the Hyd−AuNP−Apt bioconjugate. To confirm the function of hydrazine, a control experiment was performed under the same conditions by using AuNP−Apt/HER2/anti-HER2/poly-DPB-(AuNP)/GC without hydrazine. In this case, no peaks are observed between +0.4 and −0.4 V (curve 2 of the inset in Figure 2) in the cyclic voltammogram. Even after the interaction with a silver nitrate solution, the cyclic voltammogram recorded for the control does not exhibit any redox peaks corresponding to the Ag/Ag^{I} couple (Figure 2b). These results clearly show that hydrazine specifically reduces the silver ion to silver metal onto the Hyd−AuNP−Apt bioconjugate. Compared to the current response generated by hydrazine only (curve 1 of the inset in Figure 2), the current is amplified 50-fold by the deposited silver. This clearly shows that the signal has been significantly improved due to the deposition of silver, which would certainly contribute to the ultrasensitive detection of HER2. In another control experiment we used only a Hyd−AuNP conjugate, where no signal was obtained. This was due to the absence of aptamer, which selectively binds to the HER2 antigen captured by the anti-HER2/poly-DPB(AuNP)/GC probe. This suggests that the present method is highly selective toward HER2 detection and is accurate for the quantitative measurement. The quantity of deposited silver is dependent on the amount of the Hyd−AuNP−Apt bioconjugate, which strictly depends on the concentration of HER2. As a result, the nonspecific deposition of silver is avoided, and the accuracy of the sensor is improved. On the basis of the cyclic voltammogram of silver-deposited Hyd−AuNP−Apt/HER2/anti-HER2/poly-DPB(AuNP)/GC, square wave stripping voltammograms were recorded from 0.0 to 0.6 V during stripping of the deposited silver for the detection of HER2 and HER2-overexpressing SK-BR-3 breast cancer cells.

Optimization of Analytical Parameters and HER2 Detection. To determine the optimal analysis conditions for the sensor, the experimental parameters that could affect the sensor response were optimized in terms of the anti-HER2 concentration, pH, immune reaction time, and temperature (Figure S2, Supporting Information). During optimization of the anti-HER2 concentration, different concentrations of anti-HER2 (10, 50, 100, 150, 200, 250, and 300 μg/mL) were incubated overnight with the activated poly-DPB(AuNP)/GC. After being washed with PBS, the anti-HER2-immobilized probe sequentially interacted with HER2, the Hyd−AuNP−Apt bioconjugate, and the silver nitrate solution. After washing, square wave stripping voltammograms were recorded for the silver-deposited Hyd−AuNP−Apt/HER2/anti-HER2/poly-DPB(AuNP)/GC in 0.1 M PBS. The effect of the anti-HER2 concentration on the sensor response is shown in Figure S2A. The current response increased with increasing concentrations of anti-HER2. However, when the anti-HER2 concentration was 200 μg/mL, there was no significant increase in the response because of the saturation of the active sites for immobilizing anti-HER2. Therefore, the 200 μg/mL concentration of anti-HER2 was used for the sensor probe preparation. To investigate the effect of the pH on the current response, square wave stripping voltammograms for the silver-deposited Hyd−AuNP−Apt/HER2/anti-HER2/poly-DPB(AuNP)/GC were recorded in 0.1 M PBS with pH values varying from 6.0 to 7.6. The current increased as the pH increased from 6.0 to 7.0 and then decreased at pH higher than 7.0 (Figure S2B). The low response at lower pH was attributed to the instability of the immunoreaction. The decrease of response in basic environments might be due to the formation of silver phosphate, which exhibited weak solubility in water and covered the sensor surface to block the subsequent stripping of silver to silver ion. The maximum current was observed at a pH of 7.0. Therefore, all subsequent experiments were performed in 0.1 M PBS with a pH of 7.0. The effect of the immune reaction time between anti-HER2 and HER2 was investigated between 1.0 and 30.0 min (Figure S2C). As the immune reaction time increased from 1.0 to 20.0 min, the current responses increased. The current response did not increase over 20.0 min possibly due to the saturation effect. Thus, 20.0 min was selected as the optimal immune reaction time. In addition, the effect of temperature on the current response was investigated between 10 and 60 °C.

dx.doi.org/10.1021/ac302923k | Anal. Chem. 2013, 85, 1058−1064

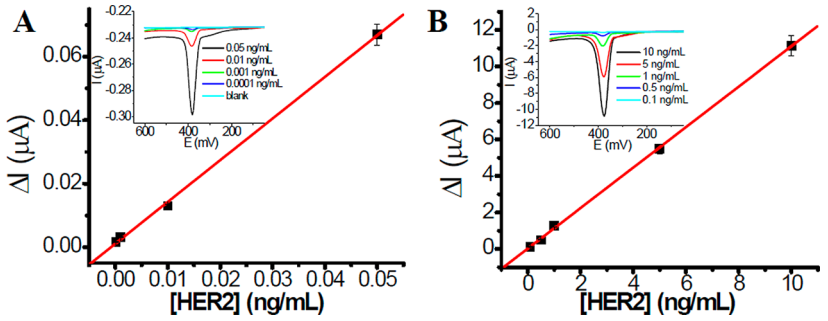

Figure 3. Calibration curves for the immunosensor in the range of (A) 0.0001−0.05 ng/mL and (B) 0.1−10 ng/mL. The insets show the corresponding square wave stripping voltammograms for varied HER2 concentrations.

The current increased as the temperature increased from 15 to 40 °C and then suddenly decreased at temperatures over 40 °C because of damage to the immunocomplex (as shown in Figure S2D). Therefore, 40 °C was selected as the optimal temperature.

Under the optimized conditions, the anti-HER2/poly-DPB(AuNP)/GC probe was used to detect various concentrations of HER2 in 25-fold-diluted human serum, and it sequentially reacted with the Hyd−AuNP−Apt bioconjugate and the silver nitrate solution. After washing, square wave stripping voltammograms were recorded for the silver-deposited Hyd−AuNP−Apt/HER2/anti-HER2/poly-DPB-(AuNP)/GC probe in 0.1 M PBS. A gradual increase in the current was observed when the HER2 concentration increased from 0.1 pg/mL to 10 ng/mL (insets of Figure 3). The corresponding calibration curves are shown in Figure 3, which demonstrate good linearity in a dynamic range between 0.1 pg/mL and 10 ng/mL HER2. The linear dependency of the HER2 analysis yields the equation $-i_p$ (μA) = (0.012 ± 0.002) + (1.117 ± 0.008){[HER2] (ng/mL)}, with a correlation coefficient of 0.9998. The sensitivity of the sensor is 1.117 ± 0.008 μA mL ng^{-1}, which is 50-fold higher than that given in the previous report for use of silver enhancement for biomolecular detection.[13] On the basis of five measurements for the standard deviation of the blank noise (95% confidence level, k = 3, n = 5), the HER2 detection limit is determined to be 0.037 ± 0.002 pg/mL, which is much lower than that previously reported.[25] The relative standard deviation is less than 5%, indicating good reproducibility of the proposed sensor.

In Vitro Detection of Cells and Direct Microscopic Analysis. We also applied this method for the quantitative in vitro detection of SK-BR-3 breast cancer cells in the human serum samples. Different concentrations of SK-BR-3 breast cancer cells, ranging from 10 to 40 000 cells/mL, were dispersed into 25-fold-diluted human serum, incubated on the proposed anti-HER2/poly-DPB(AuNP)/GC probe, combined with the prepared Hyd−AuNP−Apt bioconjugate, and reacted with silver nitrate. To investigate the change in the morphology of the SK-BR-3 cell surface, SEM images were collected both before and after silver deposition. As shown in Figure 4, the surface of the cell captured by the anti-HER2/poly-DPB-(AuNP)/GC probe is smooth and clean (image a). However, after treatment of the Hyd−AuNP−Apt bioconjugate and silver nitrate, the cell surface becomes rough and the cell size becomes larger due to bioconjugate binding and silver deposition, respectively (image b). It is interesting to note that the background of the image remains the same in both cases, indicating that there is no cross-reactivity and

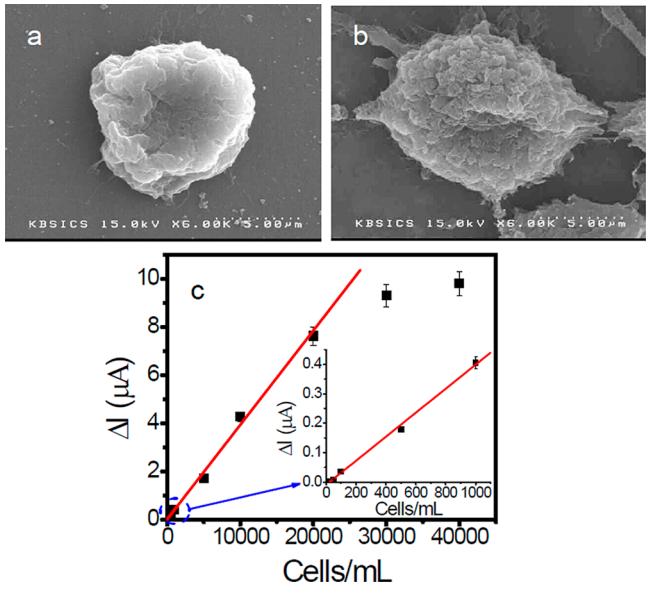

Figure 4. SEM images of the probe-captured SK-BR-3 breast cancer cell before (a) and after (b) bioconjugate binding and silver deposition. (c) Current responses of the sensor toward varied concentrations of SK-BR-3 breast cancer cells.

bioconjugate binding and silver deposition are extremely specific. To quantitatively analyze the deposited silver, square wave stripping voltammograms were obtained in 0.1 M PBS. The effect of the SK-BR-3 cell numbers on the current response is shown in Figure 4c. The current response increases with increasing numbers of SK-BR-3 breast cancer cells. The corresponding calibration plot exhibits linearity in the range between 50 and 20 000 cells/mL. However, at higher numbers over 25 000 cells/mL, the current response is almost steady; this is because the binding site is saturated by the captured cells. The detection limit of SK-BR-3 breast cancer cells is determined to be 26 cells/mL on the basis of five measurements for the standard deviation of the blank noise (95% confidence level, k = 3, n = 5). The obtained detection limit is better than the previously reported detection limit of 40 cells/mL using optical methods for the detection of SK-BR-3 breast cancer cells.[5] This detection limit is also lower than that of the previously reported conventional immunoassay method for cell detection using $AgNO_3$/hydroquinone reduction medium.[26]

Selectivity and Precision of Analysis. The selectivity for the in vitro detection of SK-BR-3 cancer cells was also studied. Figure 5 shows the microscopic images of (a) SK-BR-3, (b) MCF 7, (c) MCF 10A, and (d) Hela cells captured by anti-

dx.doi.org/10.1021/ac302923k | Anal. Chem. 2013, 85, 1058−1064

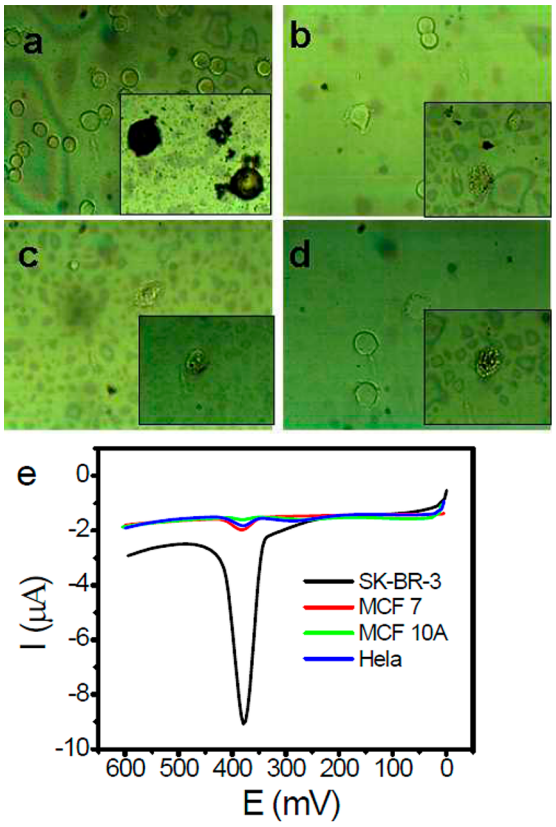

Figure 5. Microscopic images of (a) SK-BR-3, (b) MCF 7, (c) MCF 10A, and (d) Hela cells captured by anti-HER2-immobilized poly-DPB(AuNP)-coated ITO glass. The inset shows the images of the cells after deposition of silver. (e) SWSV responses of the sensors to bioconjugate-treated and silver-deposited SK-BR-3, MCF 7, MCF 10A, and Hela cells. The cell number was 20 0 00 cells/mL for each kind of cell.

HER2 that is immobilized on poly-DPB(AuNP)-coated ITO glass. The amount of captured SK-BR-3 breast cancer cells is greater than that of MCF 7 breast cancer cells, MCF 10A normal cells, and Hela cancer cells. This is because SK-BR-3 cells have overexpressed HER2 antigen and, thus, can be easily captured by the anti-HER2 probe. The insets show the images of the cells after deposition of silver. The SK-BR-3 cancer cells become black in color because of the successful deposition of silver; however, a negligible amount of black color appeared on the MCF 7 breast cancer cells, MCF 10A normal cells, and Hela cancer cells. This is because the expression of HER2 in MCF 7 breast cancer cells, MCF 10A normal cells, and Hela cancer cells is weak.[27] To confirm this observation, square wave stripping voltammograms were performed to oxidize the silver that was deposited on the cells, as shown in Figure 5e. A significantly higher response is obtained for the SK-BR-3 breast cancer cells (black curve), whereas a small response is observed for the MCF 7 breast cancer cells, MCF 10A normal cells, and Hela cancer cells, which is consistent with the microscopy results. This result demonstrates the good selectivity of the proposed sensor for the specific in vitro detection of HER2-overexpressing breast cancer cells. The high selectivity of the sensor is due to the monoclonal anti-HER2 antibody and the specific aptamer interaction toward HER2. We also confirmed the accuracy of the biosensing system for the selective detection of HER2 by performing control experiments (Figure S3, Supporting Information). Other proteins present in the real samples, such as immunoglobulins (IgG and IgM) and fibrinogens, and cancer biomarkers, such as prostate-specific antigen (PSA) and chemokine ligands (CXCL8 and CXCL5), were tested. In either case, neither the redox couple of hydrazine nor the silver stripping peak was observed. This was because the monoclonal anti-HER2 antibody and Hyd–AuNP–Apt (due to the HER2-selective aptamer) cannot bind with these protein molecules. Thus, the present method is highly selective toward HER2 detection.

CONCLUSIONS

We have developed an electrochemical sensor using the Hyd–AuNP–Apt bioconjugate for the detection of both HER2 protein and SK-BR-3 breast cancer cells for the first time. This sensor is capable of differentiating between HER2-positive breast cancer cells and HER2-negative cells. The ultrasensitivity of the developed sensor is achieved through AuNP-promoted silver enhancement. Moreover, the direct attachment of hydrazine onto the AuNP catalyst ensures the selective reduction and deposition of silver, which accurately reflects the amount of detected HER2 protein and SK-BR-3 cancer cells. Furthermore, the use of the monoclonal antibody anti-HER2 and a specific aptamer ensures the high selectivity of the sensor. In addition, the silver-stained target cells exhibit a black color and can be easily observed through a microscope, which provides a simple and convenient approach for the clinical analysis of cancer cells. This method can be easily applied for breast cancer diagnosis through either HER2 protein or breast cancer cell detection. This method can easily be adapted for the detection of other disease biomarkers and cells.

ASSOCIATED CONTENT

Supporting Information

Additional figures showing scanning electron microscopic images of the sensor probe, optimization of the experimental parameters, and selectivity and precision of analysis. This material is available free of charge via the Internet at http://pubs.acs.org.

AUTHOR INFORMATION

Corresponding Author

*Phone: (+82) 51-510-2244. Fax: (+82) 51-514-2430. E-mail: ybshim@pusan.ac.kr.

Present Address

[†]School of Chemistry and Chemical Engineering, Shandong University, Jinan, 250100, China.

Notes

The authors declare no competing financial interest.

ACKNOWLEDGMENTS

This research was supported by a National Research Foundation Grant funded by the Ministry of Education, Science and Technology, South Korea (20100029128).

REFERENCES

(1) Slamon, D. J.; Clark, G. M.; Wong, S. G.; Levin, W. J.; Ullrich, A.; McGuire, W. L. *Science* **1987**, *235*, 177–182.

(2) Owens, M. A.; Horten, B. C.; Da Silva, M. M. *Clin. Breast Cancer* **2004**, *5*, 63–99.

(3) Hung, M. C.; Schechter, A. L.; Chevray, P. Y. M.; Stern, D. F.; Weinberg, R. A. *Proc. Natl. Acad. Sci. U.S.A.* **1986**, *83*, 261–264.

(4) Telli, M, L.; Hunt, S. A.; Carlson, R. W.; Guardino, A. E. *J. Clin. Oncol.* **2007**, *25*, 3525–3533.

(5) Lu, W.; Arumugam, S. R.; Senapati, D.; Singh, A. K.; Arbneshi, T.; Khan, S. A.; Yu, H.; Ray, P. C. *ACS Nano* **2010**, *4*, 1739−1749.
(6) Li, K.; Zhan, R.; Feng, S. S.; Liu, B. *Anal. Chem.* **2011**, *83*, 2125−2132.
(7) Tsai, M. C.; Tsai, T. L.; Shieh, D. B.; Chiu, H. T.; Lee, C. Y. *Anal. Chem.* **2009**, *81*, 7590−7596.
(8) Gao, J.; Chen, K.; Miao, Z.; Ren, G.; Chen, X.; Gambhir, S. S.; Cheng, Z. *Biomaterials* **2011**, *32*, 2141−2148.
(9) Moelans, C. B.; deWeger, R. A.; VanderWall, E.; vanDiest, P. J. *Crit. Rev. Oncol./Hematol.* **2011**, *80*, 380−392.
(10) Tothill, I. E. *Semin. Cell Dev. Biol.* **2009**, *20*, 55−62.
(11) Burdall, S. E.; Hanby, A. M.; Lansdown, M. R.; Speirs, V. *Breast Cancer Res.* **2003**, *5*, 89−95.
(12) Taton, T. A.; Mirkin, C. A.; Letsinger, R. L. *Science* **2000**, *289*, 1757−1760.
(13) Wan, Y.; Wang, Y.; Wu, J.; Zhang, D. *Anal. Chem.* **2011**, *3*, 648−653.
(14) Karin, Y.; Torres., C.; Dai., Z.; Rubinova, N.; Xiang, Y.; Pretsch, E.; Wang, J.; Bakker, Y. *J. Am. Chem. Soc.* **2006**, *128*, 13676−13677.
(15) Hacker, G. W. In *Colloidal Gold: Principles, Methods, and Applications*; Hayat, M. A., Ed.; Academic Press: San Diego, CA, 1989; Vol. *1*, Chapter 10.
(16) Zehbe, I.; Hacker, G. W.; Su, H.; Hauser-Kronberger, C.; Hainfeld, J. F.; Tubbs, R. *Am. J. Pathol.* **1997**, *5*, 1553−1561.
(17) Nickel, U.; Castell, A.; Poppl, K.; Schneider, S. *Langmuir* **2000**, *16*, 9087−9091.
(18) Koh, W. C.; Son, J. I.; Choe, E. S.; Shim, Y.-B *Anal. Chem.* **2010**, *24*, 10075−10082.
(19) Kim, M. Y.; Jeong, S. *Nucleic Acid Ther.* **2011**, *21*, 173−178.
(20) Zhu, Y.; Chandra, P.; Song, K. M.; Ban, C.; Shim, Y.-B. *Biosens. Bioelectron.* **2012**, *36*, 29−34.
(21) Chandra, P.; Noh, H. B.; Won, M.-S.; Shim, Y.-B. *Biosens. Bioelectron.* **2011**, *26*, 4442−4449.
(22) Shiddiky, M. J. A.; Rahman, M. A.; Shim, Y.-B. *Anal. Chem.* **2007**, *79*, 6886−6890.
(23) Zhu, Y.; Son, J. I.; Shim, Y.-B. *Biosens. Bioelectron.* **2010**, *26*, 1002−1008.
(24) Noh, H. B.; Rahman, M. A.; Yang, J. E.; Shim, Y.-B. *Biosens. Bioelectron.* **2011**, *26*, 4429−4435.
(25) Loo, L.; Capobianco, J. A.; Wu, W.; Gao, X.; Shih., W. Y.; Shih, W. H.; Pourrezaei, K.; Robinson, M. K.; Adams, G. P. *Anal. Chem.* **2011**, *83*, 3392−3397.
(26) Wan, Y.; Wang, Y.; Wu, J.; Zhang, D. *Anal. Chem.* **2011**, *83*, 648−653.
(27) Neve, R. M.; Chin, K.; Fridlyand, J.; Yeh, J.; Baehner, F. L.; Fevr, T.; Clark, L.; Bayani, N.; Coppe, J. P.; Tong, F.; Speed, T.; Spellman, P. T.; DeVries, S.; Lapuk, A.; Wang, N. J.; Kuo, W. L.; Stilwell, J.; Pinkel, D.; Albertson, D. G.; Waldman, F. M.; McCormick, F.; Dickson, R. B.; Johnson, M. D.; Lippman, M.; Ethier, S.; Gazdar, A.; Gray, J. W. *Cancer Cell* **2006**, *10*, 515−527.